Atmospheric
Chemistry
and Physics

Air mass history linked to the development of Arctic mixed-phase clouds

Rebecca J. Murray-Watson and Edward Gryspeerdt

Department of Physics, Imperial College London, London, SW7 2BX, UK

Correspondence: Rebecca J. Murray-Watson (rebecca.murray-watson17@imperial.ac.uk)

Abstract. Clouds formed during marine cold-air outbreaks (MCAOs) exhibit a distinct transition from stratocumulus decks near the ice edge to broken cumuliform fields further downwind. The mechanisms associated with ice formation are believed to be crucial in driving this transition, yet the factors influencing such formation remain unclear. Through Lagrangian trajectories collocated with satellite data, this study investigates the development of mixed-phase clouds using these outbreaks. Cloud formed in MCAOs are characterized by a swift shift from liquid to ice-containing states, contrasting with non-MCAO clouds also moving off the ice edge. These mixed-phase clouds are predominantly observed at temperatures below $-20\,°C$ near the ice edge. However, further into the outbreak, they become dominant at temperatures as high as $-13\,°C$. This shift is consistent with the influence of biological ice-nucleating particles (INPs), which become more prevalent as the air mass ages over the ocean. The evolution of these clouds is closely linked to the history of the air mass, especially the length of time it spends over snow- and ice-covered surfaces – terrains may that be deficient in INPs. This connection also accounts for the observed seasonal variations in the development of Arctic clouds, both within and outside of MCAO events. The findings highlight the importance of understanding both local marine aerosol sources near the ice edge and the overarching INP distribution in the Arctic for modelling of cloud phase in the region.

1 Introduction

Marine cold-air outbreaks (MCAOs) are formed when cold-air masses from continental or sea ice sources are advected over the relatively warm ice-free ocean surface, sometimes in the wake of extratropical cyclones (Brümmer, 1999; Kolstad et al., 2009; Fletcher et al., 2016a). Due to the strong winds and the temperature contrast between the cold, dry air and the comparatively warm ocean surface, significant latent and sensible heat fluxes are generated, which can be some of the strongest on Earth ($100\,s$ and $1000\,W\,m^{-2}$; Shapiro et al., 1987; Renfrew and Moore, 1999; Papritz and Spengler, 2017; Aemisegger and Papritz, 2018; Lackner et al., 2023). MCAOs are relatively common occurrences in the Arctic in all seasons except summer (Fletcher et al., 2016a). The instability caused by the turbulent heat fluxes triggers shallow roll convection and a deepening of the boundary layer, which promotes cloud formation. These clouds have distinctive mesoscale organization and development, transforming from overcast cloud streets to broken cumuliform cloud fields with increasing fetch across the ocean (Hartmann et al., 1997; Brümmer, 1999; Pithan et al., 2018). The clouds on either side of the transition have distinct properties; in particular, the post-transition clouds typically have a weaker shortwave cooling effect (McCoy et al., 2017; Murray-Watson et al., 2023). Due to the frequency of these events in the Arctic, it is possible that changes to the cloud development could impact the radiative effect of these clouds and in turn modulate the Arctic surface energy budget. As the Arctic is changing rapidly (IPCC, 2021), elucidating the influences on the energy budget is key to understanding the effects of climate change on the region.

Precipitation is thought to be crucial to the transition; as precipitation sublimates or evaporates, it cools the sub-cloud layer. This creates a temperature inversion and triggers decoupling of the surface, which eventually leads to the cloud break-up (Abel et al., 2017; Yamaguchi et al., 2017). Pre-

cipitation reduces the water content within the cloud, further contributing to the cloud's dissipation. Therefore, processes which affect precipitation, such as aerosol concentrations, are likely to affect the transition (Murray-Watson et al., 2023). Ice formation is hypothesized to enhance precipitation and may accelerate the transition from the stratocumulus to cumulus clouds in outbreaks (Tornow et al., 2021). However, the factors which affect the formation and evolution of ice in these clouds are highly uncertain, in part due to a lack of in situ observations in the region.

Vergara-Temprado et al. (2018) determined that the lifetime of the stratocumulus regime was influenced by the concentration of ice-nucleating particles (INPs). Prolonged stratocumulus coverage was observed under low-INP conditions, while high INP concentrations resulted in a broken cumulus clouds, leading to significant reductions in the shortwave cooling. Flight campaign measurements of clouds in MCAOs indicate that there is typically little ice in the stratocumulus regime and substantially more ice in the cumulus clouds (Abel et al., 2017; Lloyd et al., 2018). However, this shift to a more glaciated cloud regime cannot be entirely explained by the presence of INPs; Abel et al. (2017) observed a rapid enhancement of ice crystal number concentration that was not matched by the ambient INP availability. Therefore, secondary ice production, in which an ice crystal is formed from an existing ice crystal, might be necessary to explain the development of ice-containing clouds observed in these outbreaks.

One of the most well-known secondary ice production processes is known as the Hallett–Mossop mechanism. This is the process by which ice splinters are produced following the riming of a supercooled droplet onto an existing ice particle (Hallett and Mossop, 1974). These ice splinters themselves can rime onto droplets and produce more ice, therefore reducing the dependence on INPs for ice formation. The process is most efficient between -3 and $-8\,°C$ and for droplets with a diameter greater than $24\,\mu m$ or less than $13\,\mu m$ (Mossop, 1978, 1985; Heymsfield and Mossop, 1984). The enhanced ice crystal concentration observed in Abel et al. (2017) occurred in lower-level cumuliform clouds which had cloud base temperatures within the Hallett–Mossop temperature range, suggesting that this mechanism was active. Through modelling, they found that this enhanced precipitation from this secondary ice production was essential for the stratocumulus-to-cumulus transition. Surface-based radar observations from the Cold-Air Outbreaks in the Marine Boundary Layer Experiment (COMBLE) field campaign (Geerts et al., 2022) also found evidence of secondary ice production in MCAO clouds in the Hallett–Mossop temperature range, with ice multiplication factors on the order of 100 (Mages et al., 2023). Although there is still uncertainty about the physical mechanism of the Hallett–Mossop process, it is one of the only secondary ice production mechanisms parameterized in weather and climate models.

Riming, or the freezing of supercooled droplets onto ice crystals, is also thought to influence MCAO transitions. Abel et al. (2017) found rimed graupel particles in the pre- and post-transition clouds. Tornow et al. (2021) suggested a mechanism called "preconditioning by riming", during which the formation of ice precipitation primes the MCAO clouds for transitioning. By reducing the cloud water, scavenging aerosols, and cooling the sub-cloud layer, increasing ice concentrations accelerated the cloud break-up.

Even given the importance of secondary ice production, it is evident that sources of INPs in the region have a strong control on MCAO cloud development. However, there is great uncertainty about INPs globally due to the diversity of sources, variety of physicochemical properties, low concentrations, and seasonal cycle (Murray et al., 2012, 2021). This is particularly true in the Arctic, where INP concentration are much lower than the global average (Li et al., 2023), as sparse measurements contribute to a greater lack of knowledge (Schmale et al., 2021). However, a number of field campaigns or in situ measurements have identified the Arctic ocean as a source of biological INPs (Bigg, 1996; Bigg and Leck, 2001; Irish et al., 2017, 2019; Creamean et al., 2019; Hartmann et al., 2021; Porter et al., 2022; Li et al., 2023). This organic matter is transported from the sea surface to the atmosphere via a bubble-bursting mechanism (Wilson et al., 2015). Wex et al. (2019) identified a seasonal cycle to INP availability around the Arctic, with higher concentrations in the summer months, likely due to enhanced biological activity spurred by increased availability of sunlight. Biological INPs are distinctive as they can cause ice formation at higher temperatures compared to other INPs such as mineral dust and are typically the dominant INPs active above $-15\,°C$.

Several studies have explored the influence of long-distance transport and the length of time an air parcel remains over various surface types on the INPs present in those air masses. Porter et al. (2022) found that in the summer-time high Arctic, the presence of high-temperature INPs was associated with air parcels that had spent time over land or ocean. In contrast, time over the sea ice was associated with low aerosol concentrations (Mauritsen et al., 2011). Similarly, Irish et al. (2019) found a positive correlation between INP concentration and time over snow-free land surface and a negative correlation with time spent over pack ice. However, they found a weakly negative relationship between INP concentrations and time spent over the open ocean. Li et al. (2023) also found low-INP populations in air masses which travelled over the sea ice and that long-range dust from Arctic sources such as Greenland was associated with particularly high INP concentrations. Bigg (1996) linked the time since the air parcel had been over the open ocean to declining INP concentrations, suggesting that the marine sources dominated INP concentrations. In contrast to many of these studies, Hartmann et al. (2021) found no connection between INP concentrations and air mass history and determined that the observed marine biological INPs were produced locally.

MCAOs have proven a challenge to model due to the difficulties in capturing the complex system dynamics. Even higher-resolution numerical weather prediction (NWP) models struggle due to a lack of knowledge around mixed-phase processes and the clouds falling into a convective grey zone, where the necessary dynamics cannot be parameterized (Field et al., 2017). These shortcomings lead to biases between NWP-modelled cloud properties and observations of cloud water path and cloud fraction in the stratocumulus regime in MCAOs, leading discrepancies in radiative properties (Field et al., 2017). Improving the cloud microphysics scheme, in particular the ice formation processes at warmer temperatures, can lead to a better representation of MCAO clouds, but biases still exist (Field et al., 2014). Poor representation of ice processes in models causes the rapid depletion of liquid, leading to an earlier breakdown of stratocumulus clouds than observed and lower amounts of supercooled water (Abel et al., 2017; Van Weverberg et al., 2023). In the Southern Ocean, the inability to represent supercooled water in MCAO clouds has been identified as a central factor contributing to biases in shortwave radiation (Bodas-Salcedo et al., 2014, 2016). In general, mixed-phase clouds are challenging to model due to the complexity of physical processes associated with their formation and maintenance and a lack of observations of fundamental mechanisms, which lead to uncertain parameterizations (Morrison et al., 2012). Similarly to the MCAO-specific cases, Cesana et al. (2022) found that general circulation models (GCMs) which have more complex microphysics schemes typically produce better simulations of the liquid-to-ice ratio in mixed-phase clouds in the Southern Ocean than simpler schemes. As mixed-phase clouds are central to the Arctic energy budget (Shupe and Intrieri, 2004) and may prove important components of the cloud radiative feedbacks (Tan and Storelvmo, 2019), targeting the uncertainty surrounding them is key to improving future projections of the Arctic climate.

It is evident that an advanced understanding of the formation of ice in cold-air outbreak clouds is required to improve the modelling deficiencies. There have been several observational campaigns targeting cold-air outbreak clouds, such as the recent COMBLE campaign in the north European Arctic (Geerts et al., 2022) and HALO-(AC)[3] flight campaign. However, many of the observational studies are limited in space or time and therefore provide a relatively limited picture of the cloud development. Satellites can overcome some of these challenges, and while they do not provide as high-resolution data as the in situ studies, they offer the opportunity to capture the spatial and temporal dynamics of cold-air outbreak clouds on a much larger scale. Previous studies typically have relied on snapshot satellite imagery to investigate the prevalence of ice-containing clouds in MCAOs (e.g. Fletcher et al., 2016b), despite these properties depending on the stage of the outbreak's progression, as ice is more likely to be found in post-transition cumuliform clouds (Abel et al., 2017).

In this work, we target the uncertainty surrounding the development of mixed-phase clouds in MCAOs. In particular, we address two aspects of mixed-phase development: (i) the temporal scales over which the mixed-phase clouds form and the dependence on temperature and (ii) the role that air mass history may play in the types of INPs available for ice formation. To achieve this, we use a novel method of creating a series of trajectories of air parcels moving from the sea ice and across the open ocean. We collocate these trajectories with active remote sensing data to create a composite picture of the temporal development of mixed-phase clouds during these outbreaks. We also consider clouds which transition from the ice edge to the ocean but are not embedded in an outbreak to study the influences on general mixed-phase clouds in the region. To investigate the relative importance of local aerosols versus distant INP sources, we examine the origin of the air mass and the types of surfaces it has passed over before reaching the pack ice. We find that in most MCAOs, the proportion of mixed-phase clouds typically rapidly increases as the cloud moves from the ice edge. These mixed-phase clouds initially form at low temperatures but eventually become dominant at around $-13\,°C$, consistent with marine INPs being transported to the cloud layer. We present evidence linking the air mass history and aerosol availability to the formation of mixed-phase clouds in MCAO and non-MCAO clouds. These results highlight the crucial role of INPs in cloud development and the need for more detailed knowledge of their sources in the region to be able to accurately model mixed-phase cloud development.

2 Methods

2.1 Calculating time since ice

This work uses Lagrangian trajectories to study the temporal evolution of the cloud phase in cold-air outbreaks. A detailed discussion of the trajectory generation is provided in Murray-Watson et al. (2023), which in turn is adapted from Horner and Gryspeerdt (2023). In summary, hourly ERA5 (ECMWF Reanalysis v5; Hersbach et al., 2020) 1000 hPa wind data are used to advect pixels forward through time. When a pixel transitions over the sea ice edge (data from Nimbus-7 SMMR and DMSP SSM/I-SSMIS version 2 product; DiGirolamo et al., 2022), the pixel receives a time since ice (TSI) increment of 1 h. This process is iterated for each time step, so pixels have a value of 1 added to the TSI for each hour they remain over the ocean since leaving the ice edge (so pixels move from being 1 to 2 h since ice and so on). These TSI trajectories allow for the movement of air parcels to be tracked over the ocean after leaving the sea ice edge. When these trajectories are collocated with satellite data, they can provide insights into the progression of these outbreaks. A series of reverse trajectories are also generated, measuring instead the time until an air parcel reaches the ice edge, moving towards the ice (as in Murray-Watson et al., 2023). These "Towards"

trajectories allow for a comparison between the clouds moving off the ice edge and other clouds in the region, including clouds formed in warm-air intrusions, revealing the impact of any undetected sea ice on the cloud retrievals. Only the North Atlantic and Kara Sea regions were considered to prevent bias being introduced from short trajectories (Murray-Watson et al., 2023), and a period of 7 years of data was included (2008–2014).

This work considers an extension to the trajectory method described in Murray-Watson et al. (2023) by examining the duration of time a given air parcel spends over the sea ice and snow-covered surfaces before it leaves again and moves over the open ocean. Previous work suggests that the duration spent over the sea ice can change the air mass properties and the types of clouds formed (Silber and Shupe, 2022). In the high Arctic, the boundary layer above the pack ice can be extremely clean, with measurements of cloud condensation nuclei concentration recorded below $1\,\text{cm}^{-3}$ during the Arctic Summer Cloud Ocean Study (ASCOS) campaign (Mauritsen et al., 2011) and previous work linking air mass history to INP concentrations (Irish et al., 2019; Porter et al., 2022). The method for time over sea ice/land is similar to that above but instead considers all pixels above $50°\,\text{N}$ in order to better capture the air mass history, including air moving into the Arctic region. The surface type data are obtained from the Interactive Multisensor Snow and Ice Mapping System (IMS) Daily Northern Hemisphere Snow and Ice Analysis at 1 km resolution version 1 product (U.S. National Ice Center, 2008) and are regridded to the same polar stereographic, 25 km by 25 km grid as the sea ice data. Land without snow and snow-covered land were used to define land pixels. If a pixel contains a mix of surface types, it is categorized under the dominant type when this type occupies more than 75 % of the pixel area. Otherwise, the pixel is characterized as uncertain.

2.2 MCAO index

The MCAO index (M), which is an indicator of the instability of the boundary layer, is calculated as

$$M = \theta_{\text{skt}} - \theta_{800}, \tag{1}$$

with θ_{skt} and θ_{800} as the potential temperatures of the surface skin and 800 hPa, respectively (Kolstad and Bracegirdle, 2008; Fletcher et al., 2016b). The temperature data are obtained from ERA5 and processed into the same grid as the wind data. An outbreak is defined as $M > 0$, with increasingly negative values indicative of greater boundary layer stability. MCAOs are relatively common in the region and form an important part of the high-latitude weather system, particularly in the non-summer months (Fletcher et al., 2016b).

2.3 Cloud properties

Cloud-phase data were from DARDAR v2 (raDAR/liDAR; Delanoë and Hogan, 2010; Ceccaldi et al., 2013), which is produced using lidar data from CALIOP (Winker et al., 2009) and radar data from CloudSat (Stephens et al., 2008). As the radar can penetrate optically thick clouds and is sensitive to larger particles and the lidar is sensitive to thin clouds and smaller particles, this allows for a wider variety of clouds to be studied than if the datasets were used in isolation. As the lidar data are produced at a higher resolution than Cloud-Sat, several CALIOP retrievals are matched to each radar retrieval when merged, resulting in a vertical resolution of 60 m and a horizontal resolution of 1.1 km. The phase determination algorithm incorporates data from the CALIOP L1B attenuated backscatter profiles, the CALIOP L2 vertical feature mask, the CloudSat 2B-GEOPROF radar, and ECMWF-AUX temperature data. Cases with the cloud top height below 720 m are excluded due to surface clutter affecting the radar retrievals, as in other studies (e.g. Kay and Gettelman, 2009). The phase fraction for each profile is calculated as the number of DARDAR retrievals for each flag divided by the number of DARDAR retrievals for each 25 km by 25 km TSI grid box. For this study, the ice category comprises the DARDAR phase flags Ice, Spherical_or_2D_ice, and Highly_concentrated_ice, and the DARDAR flag Supercooled_and_ice is considered mixed phase. We adopt the method of defining mixed-phase profiles in DARDAR from Danker et al. (2022): if a mixed layer is above an ice layer, a supercooled layer above an ice layer, any combination of supercooled and mixed layers, or any combination of supercooled or mixed above ice layers are classified as mixed-phase clouds. The warm liquid and supercooled liquid DARDAR categories are combined to create a single liquid category. Multi-layer clouds are excluded by removing profiles which have more than three clear-sky or failed retrievals (equating to a distance of 240 m) between cloud layers, as in previous work (Danker et al., 2022). Clouds with cloud top heights recorded above 5000 m are excluded to limit the inclusion of high-level clouds not associated with MCAOs. Although this may exclude some MCAO clouds, other work has found clouds tops are typically much lower than this (Fletcher et al., 2016b; Lackner et al., 2023; Mateling et al., 2023).

Cloud effective radius (r_e) measurements were obtained from the Moderate Resolution Imaging Spectroradiometer (MODIS) Level 2 Collection 6.1 data product (MYD06_L2; Platnick et al., 2017), regridding into a 25 km by 25 km polar stereographic grid. Following Grosvenor and Wood (2014), pixels with high solar zenith angles ($> 65°$) and high viewing angles ($> 50°$) were removed due to potential biases in r_e. The dataset was filtered to include only data collocated with the DARDAR retrievals. However, MODIS filters were also used to increase confidence in the retrievals being single-layer, liquid clouds using Cloud_Multi_Layer_Flag

and Cloud_Phase_Optical_Properties. The cloud top phase was determined using the cloud optical property retrieval, which is usually in good agreement with active sensors (Marchant et al., 2016). The single-layer cloud filter also typically performs well relative to active sensors at these latitudes (Wang et al., 2016b). The MODIS cloud subpixel heterogeneity index (SPI) is the ratio of the standard deviation to the mean of the reflectance in the 0.86 μm band of the 250 m pixels which each comprise 1 km; larger values of SPI (> 30) are associated with heterogeneous cloud regimes, such as broken cumulus fields (Zhang and Platnick, 2011). In these conditions, breakdowns in the assumptions underpinning the MODIS retrievals can introduce biases (Seethala and Horváth, 2010). As such, only pixels with a low sub-pixel heterogeneity index were included (Cloud_Mask_SPI < 30; Zhang and Platnick, 2011). This reduces the dataset to approximately 40 % of its original size; while significantly reduced, this filtering is justified as it removes biased cases.

3 Results

3.1 Phase evolution as a function of time since the ice edge

Clouds created in MCAOs have a distinctive phase evolution relative to other clouds in the region (Fig. 1), most notably from the ice and mixed phases. MCAO clouds are characterized by the rapid decline of the liquid phase down to about 20 % after 6 h, with a corresponding increase in mixed-phase clouds. While the liquid fraction then remains relatively steady, the mixed phase proceeds to glaciate and convert to ice-only clouds. In contrast, for both non-MCAO and Towards clouds, the liquid phase remains dominant. The phase fractions remain relatively steady as non-MCAO clouds move off the ice edge, with nearly twice as much liquid cloud as mixed phase and very few (about 3 %) ice clouds. Although the composition of Towards clouds also shifts towards ice-containing phases as they move further north, the shift is very gradual, and liquid clouds are still dominant. This shift to mixed phase is likely in part due to decreases in cloud temperature as the clouds move towards the ice. Additionally, as these clouds move north from lower latitudes, the air masses may potentially have more INPs than the air which has spent greater lengths of time over the sea ice (discussed more in Sect. 3.4), and they therefore more readily form mixed-phase clouds. Broadly, the dominance of liquid-containing phases in the Towards clouds agrees with previous climatologies of low-level Arctic clouds (e.g. Shupe et al., 2006; Cesana et al., 2012; Yan et al., 2020) but does show more liquid-only clouds than some other studies (e.g. Shupe, 2011), although this may be due to different study regions. Using DARDAR, Fletcher et al. (2016b) also determined that clouds within outbreaks had higher ice fractions compared to other regional clouds.

This shift in MCAO clouds towards a more glaciated state is in agreement with previous observations; Abel et al. (2017) found much larger quantities of ice in the post-transition cumulus clouds relative to the upstream stratocumulus deck. The following sections explore the potential roles of the air mass history and the cloud top temperature in influencing the observed disparities in ice-containing phases between MCAO clouds and non-MCAO trajectories.

3.2 Mixed-phase development as a function of temperature and time since ice

Cloud top temperature is an important factor in the formation of ice in clouds (e.g. Korolev et al., 2003; Shupe et al., 2006; Westbrook and Illingworth, 2011; de Boer et al., 2011), typically with increasing amounts of ice at lower temperatures. However, supercooled liquid clouds have also been observed to exist at temperatures below $-15\,°C$ (e.g. D'Alessandro et al., 2021; Danker et al., 2022; Carlsen and David, 2022). Figure 2 shows evolution of the mixed-phase fraction for MCAO and non-MCAO clouds as a function of the time since ice and cloud top temperature. Mixed-phase clouds are initially only dominant at very low temperatures ($-23\,°C$) in MCAOs. As the clouds progress from the ice edge, the temperature at which the majority of clouds are mixed-phase increases, until a plateau at approximately $-13\,°C$ after 7 h. The low mixed-phase fraction at very low temperatures further into the trajectories (bottom right of Fig. 2a) is due to the shift to ice-only clouds (Supplement Fig. S1).

This is in contrast to the non-MCAO clouds; from the point of leaving the ice edge onwards, mixed-phase clouds are prevalent below $-13\,°C$ and supercooled liquid is dominant at warmer temperatures. Figure 2c underlines the differences in this initial development by emphasizing the initial relative lack of mixed-phase clouds early in MCAOs (the gradient highlighted as Region A). This gradient in the temperature at which mixed-phase clouds become the majority has previously been observed by Carlsen and David (2022), who found that the temperature at which a cloud regime switched from being liquid dominant to mixed-phase dominant (which they called T^*) increased as a function of distance from the ice edge until a plateau is reached at about $-15\,°C$. They also observed a seasonal dependence; during the summer, there was a slightly weaker gradient in T^* from the ice edge (from about -17 to $-15\,°C$) than in the winter (from about -22 to about $-15\,°C$). This may be due to the seasonal differences in MCAO events; there are relatively few MCAOs in summer (Fig. 4), so they may have been observing events more similar to Fig. 2b, i.e events which are moving off of the ice edge but are not necessarily MCAOs. Conversely, in winter, their observations match Fig. 2a more closely. The seasonal dependence of this MCAO and non-MCAO cloud evolution is discussed further in Sect. 3.4.

Figure 2a also reveals another interesting feature of the MCAO clouds; after about 7 h, a significant proportion of the
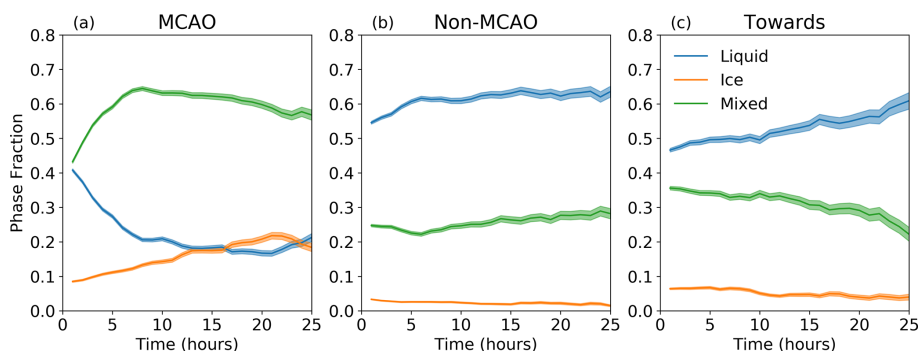
Figure 1. Evolution of cloud phase as a function of time for **(a)** MCAO, **(b)** non-MCAO, and **(c)** Towards trajectories. Note that for Towards clouds, the x axis represents hours until the clouds reach the ice edge and their development is instead read from right to left. For MCAO and non-MCAO clouds, the x axis represents time since the air parcel left the ice edge. The shading represents the 95 % confidence interval.

clouds are mixed phase at higher temperatures (between -13 and $-3\,°C$). On average, the mixed-phase proportion at these temperatures in MCAOs is 15 %–20 % greater than in non-MCAO clouds (Fig. 2c, highlighted as Region B). The potential cause of the development of these higher-temperature mixed-phase clouds in outbreaks is discussed in Sect. 4.

3.3 Environmental context

Figure 3 shows how some key environmental and meteorological variables change along the MCAO and non-MCAO trajectories to give context to the changes seen in cloud properties in subsequent sections. It can be seen that as the MCAO air parcels move off of the ice edge, they typically are very dry and clean (Fig. 3b and d). As they move further from the ice edge and over warmed surfaces, the AOD typically increases, potentially as aerosol is transported to the cloud layer (discussed further in Sect. 3.5). Further discussion of the meteorological context can be found in Murray-Watson et al. (2023).

3.4 Seasonal variability in mixed-phase development

Previous work has found a strong seasonal cycle in MCAOs, with a maximum frequency of occurrence in the winter months and a minimum in the summer months (Fletcher et al., 2016b). Figure 4, which accounts for the MCAO index just as the air parcel leaves the ice edge, shows the MCAO pixels in the Northern Hemisphere winter in the region of study are orders of magnitude less common than other seasons for the period of study.

Figure 5 shows that for most seasons, the pattern of mixed-phase cloud development in MCAOs is similar to the annual aggregate; initially, mixed-phase clouds are only dominant at very low temperatures and become increasingly dominant at higher temperatures until a plateau at around $-13\,°C$, although SON also had more mixed-phase clouds at higher temperatures later in the outbreak. JJA is an anomaly; its be-

haviour is very similar to the annual non-MCAO cloud development (Fig. 2b).

In contrast, Fig. 6 shows the seasonal development of clouds in non-MCAO events. This time, MAM, SON, and JJA replicate the annual pattern shown in Fig. 2b. However, the non-MCAO DJF mixed-phase cloud development more strongly resembles an MCAO event (Fig. 2a). A potential cause for seasonal variation in MCAO and non-MCAO mixed-phase development is discussed in Sect. 3.5.1.

3.5 Effects of air mass history

Initially focusing on the annually averaged general cases, there are several possible causes of the distinctive mixed-phase evolution in the MCAO clouds seen in Region A of Fig. 2c. One may be due to the air mass history. Figure 7a shows the duration of time that air parcels which form MCAO and non-MCAO events typically spend moving over the sea ice before crossing over to the open ocean. The pack ice is typically a poor source of INPs, with low INP concentrations being associated with longer times over ice (Porter et al., 2022; Li et al., 2023). Although AOD is an imperfect proxy for INPs, especially in a region as poorly constrained as the Arctic, Copernicus Atmosphere Monitoring Service AOD reanalysis data (Inness et al., 2019) were used to indicate the cleanliness of the air masses just as they move off of the ice edge (at a TSI $= 1$). Figure 7b indicates that these MCAO air masses typically have lower AODs than non-MCAO air masses. Therefore, as they move off the ice edge, INPs may be locally sourced from the ocean surface and transported to the cloud layer (a mechanism suggested by Fig. 3b) and then activated to form ice particles. The higher wind speeds typically observed in MCAOs (Kolstad, 2017) may aid the transport of these INPs via the bubble-bursting mechanism (Wilson et al., 2015), which has previously been observed (Inoue et al., 2021). The temperature of the liquid/mixed-phase switch (approximately $-13\,°C$ after 7 h in MCAOs) is often considered the temperature at which biological INPs tend to dominate over other poten-
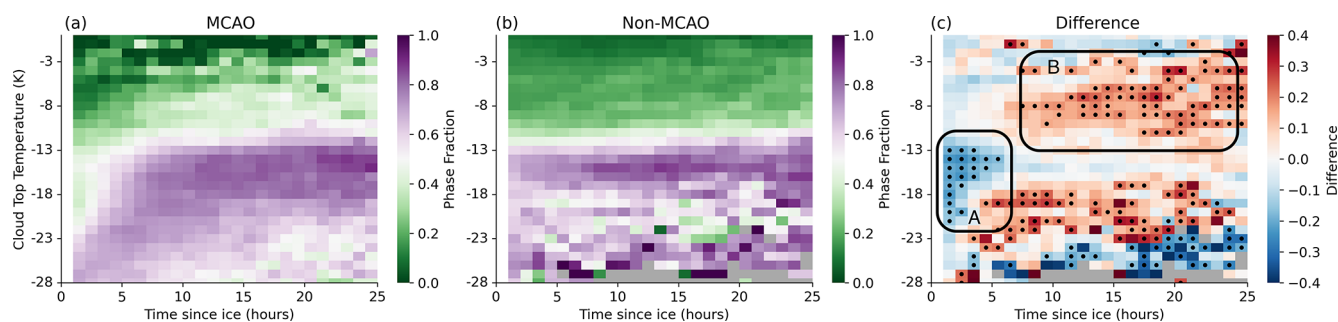
Figure 2. Evolution of mixed-phase cloud fractions as a function of time and cloud top temperature for **(a)** MCAOs and **(b)** non-MCAOs. Panel **(c)** shows the difference between panel **(a)** and panel **(b)**. Grid points with fewer than 500 successful retrievals are coloured in grey. In plot **(c)**, red indicates that there are more mixed-phase clouds in MCAOs for that given cloud top temperature and TSI than in non-MCAOs, and blue indicates the opposite. Black dots indicate significant differences based on the Mann–Whitney U test ($p < 0.05$; Mann and Whitney, 1947).
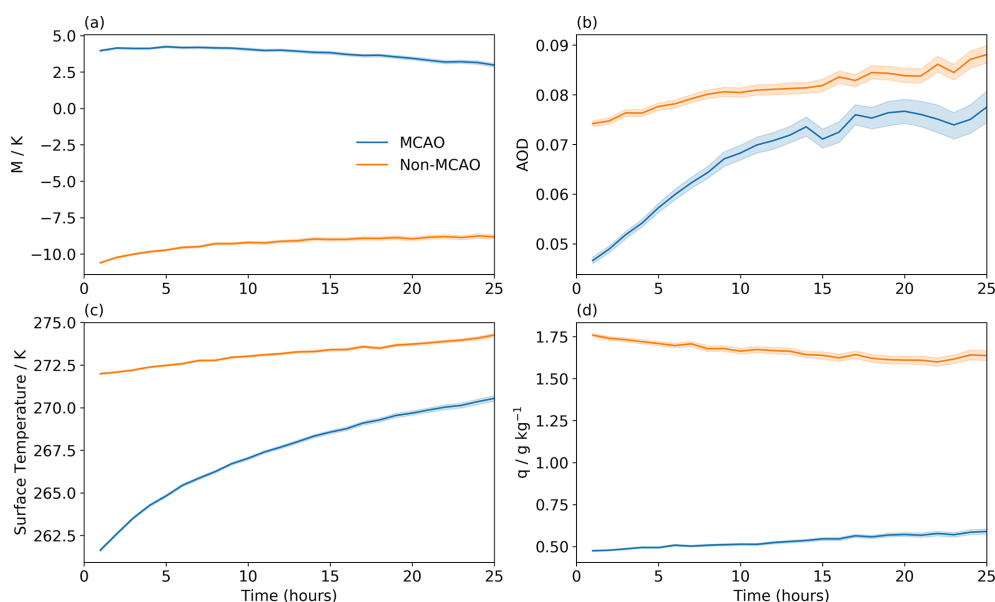
Figure 3. The average evolution of **(a)** the MCAO index, **(b)** the AOD, **(c)** the surface temperature, and **(d)** the specific humidity for MCAO and non-MCAO events. The shading represents the 95 % confidence interval.
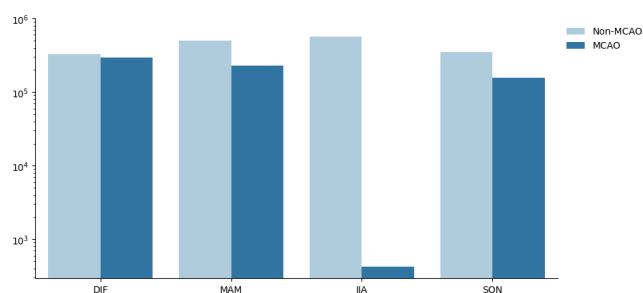
Figure 4. Number of MCAO and non-MCAO pixels recorded at TSI = 1 for each season.

tial INPs, such as mineral dust (Murray et al., 2012). Therefore, it appears that while biological INPs may already be present in the non-MCAO clouds as they move over the ice edge (indicated by the presence of mixed-phase clouds that form at −13 °C close to the ice edge), they are absent from the MCAO air masses and must be from a local source.

3.5.1 Seasonal dependence of air mass history

What causes the non-MCAO DJF clouds to develop like most MCAO clouds and MCAO JJA clouds to develop like most non-MCAO clouds? One possible explanation is that the DJF non-MCAOs are very clean, therefore causing longer times for the mixed-phase clouds to form. Similarly, we may expect the JJA MCAOs to have higher aerosol loads, therefore allowing the mixed phase to rapidly develop. In this case, we would expect the time spent over ice to be important, due to
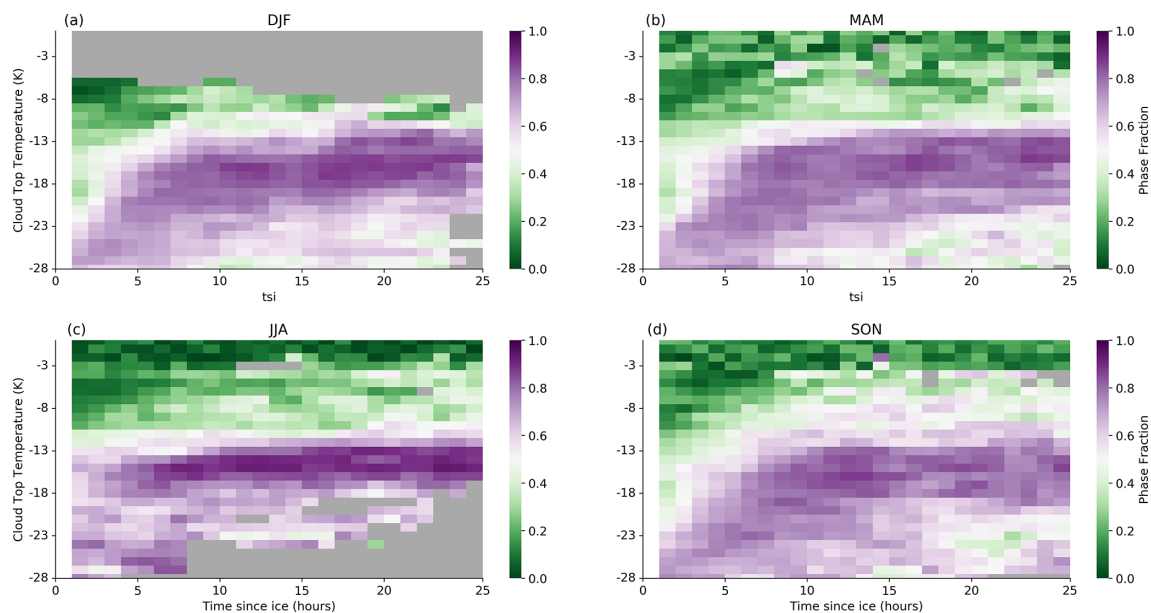
Figure 5. Evolution of cloud phase as a function of time and cloud top temperature (from the DARDAR product) for MCAO clouds in **(a)** December, January, and February; **(b)** March, April, and May; **(c)** June, July, and August; and **(d)** September, October, and November. Points for which there were fewer than 500 retrievals are coloured grey.
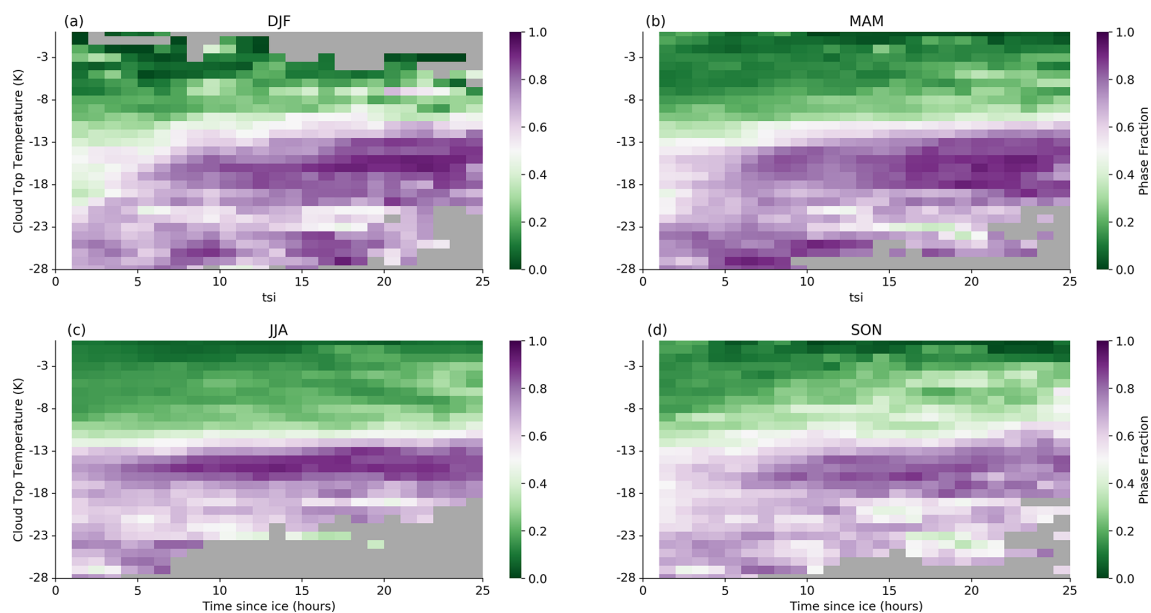

Figure 6. As Fig. 5 but for non-MCAO clouds.

the potentially cleaner air masses with longer times over ice. However, Fig. 8a shows that both DJF cases generally spend less time over ice than the other cases, contrary to what would be expected. Additionally, the JJA MCAOs spend comparable amounts of time over ice to MAM and SON cases (although, as there are fewer MCAO cases during the summer, this may be due to noise). While the CAMS AOD data (Fig. 8b) show that DJF MCAOs and non-MCAOs are both relatively clean, the SON non-MCAOs and JJA MCAOs also have similar AOD. This may be due to CAMS not capturing the types of aerosols present in SON and JJA, which are expected to be dominated by local biological sources which are absent in the DJF case.

Looking further back into the air mass history provides some potential answers. Figure 9 shows the average time that the air parcels spent over snow-covered land before
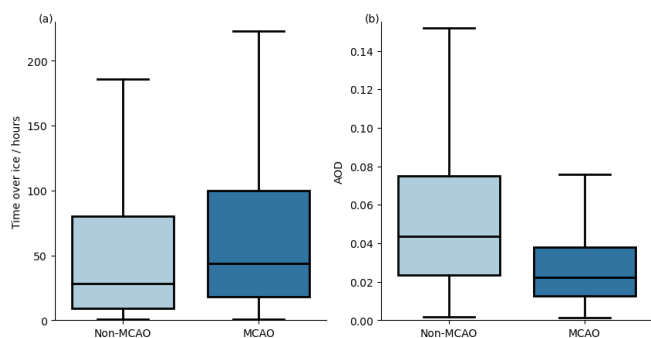
Figure 7. (a) Time spent over ice before leaving the ice edge and **(b)** AOD for MCAO and non-MCAO trajectories just as the air leaves the ice edge (at TSI = 1).
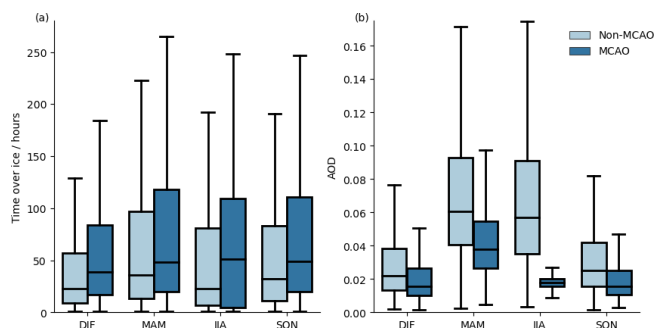

Figure 8. As Fig. 7 but broken into seasons.

Figure 9. As Fig. 8 but for time spent over snow-covered land before moving onto the ice edge.

then moving onto ice for each season. Both non-MCAO and MCAO cases in winter typically spend long times over snow-covered land before reaching the ice, while the JJA cases typically spend very little, as expected when considering the seasonal cycle of surface cover (Fig. S2). For both MAM and SON, the MCAOs usually spend a longer time over snow than non-MCAOs. Carlsen and David (2022) suggested that snow-covered surfaces prevented biological INP release and therefore suppressed mixed-phase formation at higher temperatures. Therefore, it may be that in summer, terrestrial INPs are collected from the surrounding land mass and are available, along with local, marine biological INPs, for ice formation. Terrestrial INPs have previously been found to be an important source of higher-temperature INPs in the summertime Arctic (Pereira Freitas et al., 2023). In contrast, in winter, no such INPs are available for either the MCAO events or the non-MCAO events when the air is advected over land, and therefore it takes time for the local INPs to be transported from the ocean surface to the cloud layer in both cases. Although marine biological INPs are scarcer in the winter, they are not entirely absent (e.g, Creamean et al., 2022; Hartmann et al., 2020; Pereira Freitas et al., 2023).

To test the idea that the time spent over ice- and snow-covered surfaces impacts the temperature at which mixed-phase clouds initially form through INP availability, Fig. 10 shows the development of MCAO clouds for DJF in cases
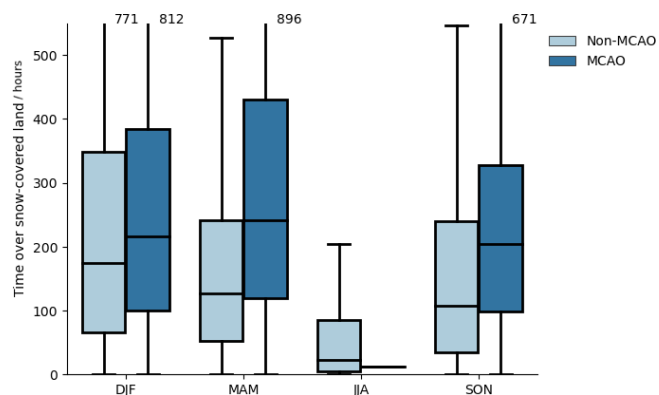
where the air parcel has spent either more or less than 2 d over these INP-limiting surfaces. As is highlighted in Fig. 10c, Region C, those cases which spend less time over sea ice form ice at higher temperatures within the first few hours over the ocean. In contrast, the cases which have spent longer times over ice are typical of the general MCAO cases, suggesting that they are devoid of higher-temperature INPs as they move off the ice edge, and these aerosols must be sourced from the ocean surface. Additionally, the difference in phase development is pronounced only at the early stages of the trajectories. At later times and lower temperatures (Fig. 10c, Region D), the phase compositions are very similar. While it should be noted that these differences are not significant at the 95 % confidence interval based on the Mann–Whitney U test, this further suggests that air mass history primarily affects the formation of mixed-phase clouds due to their reliance on INP availability.

In summary, for the initial development of ice as the cloud moves from the ice edge, the air mass history appears to influence ice formation in the MCAO and non-MCAO cases. MCAO air masses typically spend more time over ice- or snow-covered surfaces. As these surfaces may suppress the transport of INPs to the atmosphere (e.g. Carlsen and David, 2022), they may be relatively clean by the time they traverse the ice–ocean boundary. As the air moves over the ocean, the turbulent fluxes and strong wind allow for the transport of INPs to the cloud layer, allowing marine INPs to form ice. In contrast, non-MCAOs typically spend less time over these INP-blocking surfaces, allowing for non-local INPs to be carried over the ice edge and allowing for earlier mixed-phase formation. There are two exceptions: in winter, the surrounding land is covered in snow and ice, so terrestrial INPs are not available, and there is only a weak source of marine biological INPs. Additionally, the longer time spent travelling over these surfaces means that any existing INPs in the air mass are more likely to be removed without replenishment. Therefore, the wintertime non-MCAO clouds develop very similarly to the MCAO clouds. However, if the
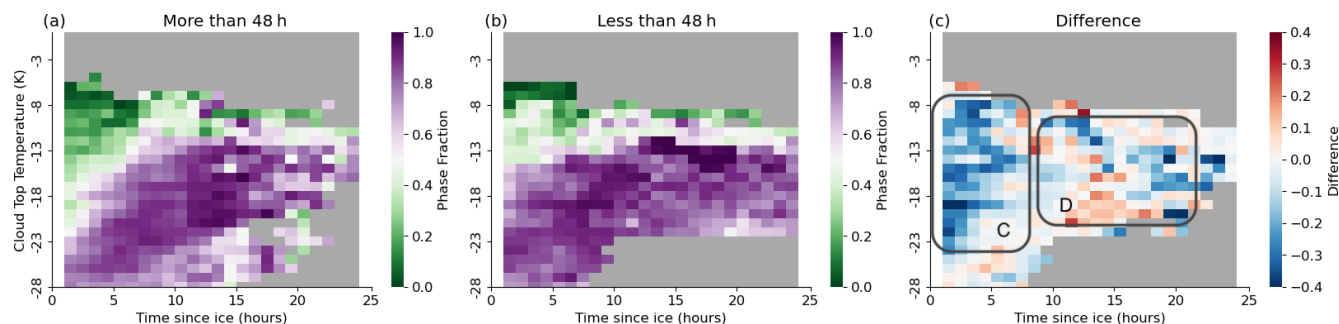
Figure 10. As Fig. 2 but for DJF MCAO cases that have spent **(a)** more than 48 h and **(b)** less than 48 h over snow- and ice-covered surfaces. Panel **(c)** shows the difference between panel **(a)** and panel **(b)**. Grid points with fewer than 250 successful retrievals are coloured in grey. Blue indicates that the cases which have spent longer times over ice have lower mixed-phase cloud fractions.

DJF air masses spend relatively little time over ice, mixed-phase clouds do form at around −13 °C close to the ice edge due to the availability of INPs. In contrast, abundant terrestrial and biological INPs in summer allow for the ready formation of ice in the MCAOs. In spring and autumn, although non-MCAO clouds do travel over ice-covered surfaces, the biological sources are still active enough to allow for quick ice formation as the clouds move from the ice edge.

4   Potential causes of the higher-temperature mixed-phase clouds

The prevalence of mixed-phase clouds with cloud top temperature (CTT) warmer than −10 °C (Region B in Fig. 2c) is challenging to explain with the data used here. There may be several causes these higher-temperature mixed-phase clouds, namely secondary ice production, the presence of INPs active at these high temperatures and potential retrieval biases, which are discussed below.

4.1   Secondary ice production

Secondary ice production has previously been cited as a cause of mixed-phase development in MCAOs; during a field campaign, Abel et al. (2017) found that the number of ice crystals in the post-transition cumuliform clouds was several order of magnitudes greater than what would be expected given the ambient INP concentrations. Mages et al. (2023) also found evidence of secondary ice production in the later stages of an outbreak. In both cases, cloud temperatures were within that of the Hallett–Mossop mechanism, and strong updrafts were recorded. The presence of moderate to strong updrafts has previously been observed to be important to the initiation of secondary ice production (Sullivan et al., 2018; Korolev et al., 2020; Luke et al., 2021). As non-MCAO clouds are not subject to the same instability as MCAO clouds and therefore do not have as strong updrafts, this may explain the absence of the mixed phase at higher temperatures. Although the mixed-phase enhance-

ment can be seen at lower temperatures than what is usual for the Hallett–Mossop temperature range (down to about −12 °C in Fig. 2c), this may be due to the fact that the cloud top temperatures are used; the cloud base would be warmer than this and therefore potentially in the appropriate temperature range. While temperatures up to −3 °C may appear relatively warm for clouds associated with MCAOs, this may be due to the satellite observing convective clouds at different stages of development, as some clouds transition through these warmer temperatures until they reach their final cloud top temperature (Lensky and Rosenfeld, 2006).

Secondary ice production is thought to be more efficient in the presence of larger liquid droplets (Rangno and Hobbs, 2001; Rosenfeld et al., 2011; Luke et al., 2021). To investigate this, the trajectories in Fig. 2a were divided into high and low r_e, based on r_e retrievals taken within 6 h of the DARDAR retrieval used in Fig. 2. The r_e data were obtained from MODIS, and due to the uncertainties associated with retrieving r_e in mixed-phase clouds (Khanal and Wang, 2018), liquid-only retrievals were used. The aim is to consider the size of liquid droplets in the cloud before they transition to a mixed-phase regime. This excludes many cases for which a liquid-only MODIS retrieval could not be made (particularly in during polar night, as MODIS requires reflected sunlight to retrieve r_e). A threshold of 14 μm was used to demarcate high and low r_e. The results are shown in Fig. 11.

Due to the seasonal bias in MODIS retrievals, the general mixed-phase development in Fig. 11 most closely resembles the JJA MCAOs (which, in turn, resembles the non-MCAO clouds). Therefore, it is uncertain how representative these results are. However, it can be seen from Fig. 11c that clouds which had larger droplets earlier in the development did go on to produce more mixed-phase clouds at the higher temperatures observed in Fig. 2. The enhancement exists across the temporal development, although it is stronger after about 7 h. Although not conclusive, this supports the argument that secondary ice production gives rise to these higher-temperature mixed-phase clouds.
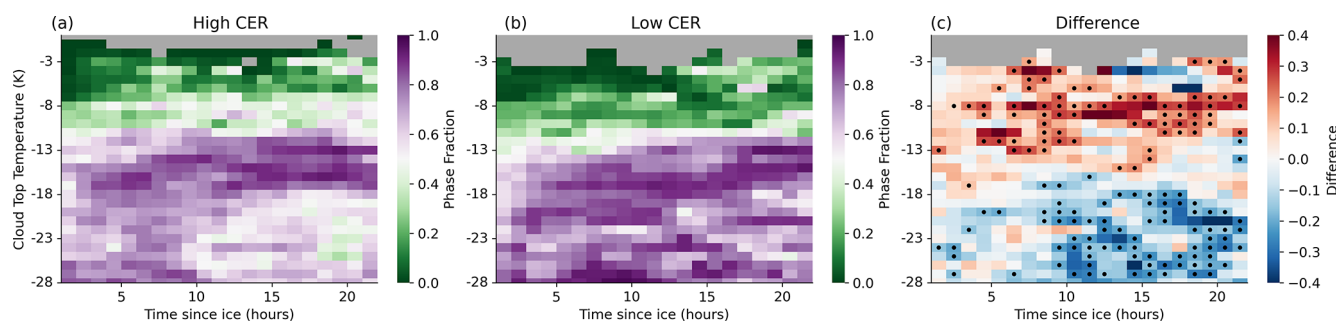
Figure 11. Evolution of mixed-phase cloud fraction as a function of time at cloud top temperature for clouds in MCAO events that have successful MODIS r_e retrievals for the liquid phase **(a)** above 14 µm and **(b)** below 14 µm. r_e retrievals must be at most 6 h before the DARDAR retrieval to be included. Panel **(c)** shows the difference between panel **(a)** and panel **(b)**. Grid points with fewer than 250 successful retrievals are coloured in grey. Note that due to data limitations this threshold is lower than for Fig. 2. Red indicates that clouds which have larger droplets earlier in the trajectory go on to have higher mixed-phase fractions than clouds which have smaller droplets. Black dots indicate significant differences based on the Mann–Whitney U test ($p < 0.05$).

4.2 Higher-temperature INPs

Another possible explanation is the activation of INPs at these higher temperatures (between -10 and $-3\,°C$). Biological INPs in the seas around the ice pack have been recorded as being active as warm as $-5\,°C$ (McCluskey et al., 2018; Irish et al., 2019; Wex et al., 2019; Li et al., 2023), albeit at low concentrations. Due to the scarcity of INPs which would nucleate ice, it may take longer for them to activate, leading to the delay in the formation of these higher-temperature mixed-phase clouds. However, as these higher-temperature INPs are biological, a strong seasonal cycle is expected; although Fig. 5 shows some seasonal differences, there is not a notable peak in summer, where biological activity is highest. Furthermore, it does not explain why this phenomenon is seen in MCAO clouds but not in non-MCAO clouds, unless the enhanced updrafts and instability in MCAOs greatly increased the transport of these INPs to the cloud layer, evidence of which has been observed previously (Inoue et al., 2021). More measurements of INPs around MCAOs would be required to determine the contribution of high-temperature biological INPs to mixed-phase cloud formation.

4.3 Retrieval biases

It is possible that the higher-temperature mixed-phase clouds are not a real effect but appear due to the radar misclassifying supercooled drizzle as ice, particularly above $-10\,°C$, due to their larger size (Zhang et al., 2017, 2018). As noted by Danker et al. (2022), this may be a particular issue with DARDAR when the lidar is attenuated in clouds with supercooled liquid tops, and heavier precipitation would be required for a CloudSat detection (Marchand et al., 2008). Drizzle has previously been observed to form in MCAOs (Abel et al., 2017; Lloyd et al., 2018), and supercooled drizzle in general has been recorded at temperatures down to

$-25\,°C$ (Silber et al., 2019). Additionally, droplets in liquid clouds formed during MCAOs grow to precipitation size (about 15 µm; Rosenfeld and Gutman, 1994), whereas those not in outbreaks do not (Murray-Watson et al., 2023), potentially explaining the differences between Fig. 2a and b. Schirmacher et al. (2023) found that CloudSat may also underestimate precipitation, particularly frozen precipitation, in outbreaks due to limitations such as surface clutter creating a blind zone for the radar close to the surface. While the COMBLE campaign, which took in situ precipitation measurements 100 s and 1000 km into these outbreaks, found that the cumuliform clouds were typically precipitating (Mages et al., 2023), with frozen precipitation being common, there is still a great deal of uncertainty about the phase of the precipitation created in these events. Therefore, it is difficult to assess how prevalent retrieval errors may be. More in situ measurements of the frequency and characteristics of supercooled drizzle would be required for a more robust understanding of precipitation in these events and to target the retrieval uncertainty.

With the data used in this work, identifying the cause of mixed-phase clouds forming above $-10\,°C$ late in the MCAO events is challenging. Some evidence such as the influence of droplet size and the absence of similar formations in non-MCAO events suggests secondary ice production, which is consistent with in situ observations of MCAO clouds. However, we cannot conclusively rule out other potential causes of the appearance of Region B in Fig. 2. Other factors, such as ice being nucleated from snow being lofted from the surface by strong winds (Geerts et al., 2015), cannot be ruled out with the current analysis. This may be especially relevant in MCAOs due to the high wind speeds, turbulence, and presence of frozen precipitation (Mateling et al., 2023). Satellite data alone are unlikely to be able to determine the formation mechanism of these late-stage mixed-phase clouds, highlighting the need for more detailed observations of this phenomenon.

5 Discussion

The results presented here are consistent with the air mass history influencing the development of mixed-phase clouds in MCAO and non-MCAO events. However, this trajectory analysis does not allow for the precise origin of the air masses to be determined, and therefore there are uncertainties in linking these trajectories to potential INP sources in the wider Arctic region. Additionally, there may be potential INP sources in the pack ice, such as open leads, which have previously been cited as aerosol sources at high latitudes (Bigg and Leck, 2001). These features may be on the order of several hundred metres in size (Wadhams et al., 1985; Li et al., 2020) and therefore below the resolution of the sea ice product (Cavalieri et al., 1996). However, Porter et al. (2022) found that open leads were very weak sources of INPs and that air that had spent time over the pack ice typically had very low aerosol concentrations. Hartmann et al. (2020) found that INPs from leads were active at high temperatures and suggested that they were from a biogenic source. Therefore, if INPs from features like open leads were prevalent in MCAOs, we may expect more mixed-phase cloud formation at higher temperatures as soon as the air moves off of the ice edge (low TSI) in Fig. 2a. As open leads cover a higher fraction of the sea ice area in summer than in winter (Lindsay and Rothrock, 1995; Wang et al., 2016a), these features may be partially responsible for the similarity between the MCAO and non-MCAO JJA cases. However, there is also a high fractional coverage of leads in the autumn, and yet the MCAO and non-MCAO development remain distinct. As there is disagreement regarding the efficacy of leads acting as INP sources, more measurements would be required to determine their influence on cloud-phase processes in the Arctic region. Whether it be through sources such as leads or INPs transported from adjacent snow-free land, these results still indicate the importance of air mass history in the formation of the mixed-phase clouds.

It should also be noted that the analysis here is based on the cloud top temperature, and the DARDAR data product derives cloud top temperature from ECMWF auxiliary data (ECMWF-AUX; Partain, 2022). This may introduce potential uncertainties. Furthermore, the DARDAR phase classification algorithm also uses the ECMWF wet bulb temperature to distinguish between ice (below $0\,°C$) and liquid or rain (above $0\,°C$), which may reduce the phase classification accuracy at higher temperatures (such the mixed-phase clouds seen in Fig. 2a). However, previous work has found good agreement between the cloud top temperature when using ECMWF-AUX temperatures and in situ radiosonde data (e.g. McErlich et al., 2021) or other retrieved satellite data (e.g. Christensen et al., 2016), so the effects of potential biases for these may be limited.

Mixed-phase clouds are of interest due to the effect of ice on the lifetime of the stratocumulus clouds, with higher INP concentrations hastening the breakdown of the high-albedo

stratocumulus deck through precipitation-related mechanisms (Vergara-Temprado et al., 2018; Murray et al., 2021; Tornow et al., 2021). However, due to limitations with Cloud-Sat in MCAOs (Schirmacher et al., 2023), DARDAR struggles to detect precipitation in these events. Therefore, we are unable to determine the effects of the formation of ice on the precipitation frequency in these clouds. Additionally, MODIS retrievals struggle with mixed-phase clouds, which are often topped by a supercooled liquid layer and therefore may be retrieved as liquid-only clouds. An analysis on the effects of ice on cloud properties and lifetime is also beyond the scope of this research. To achieve this, high-resolution measurements, both spatially and temporally, of ice formation and the effects on properties such as cloud fraction and water path would be required.

6 Conclusions and outlook

Marine cold-air outbreaks are important components of the Arctic weather system. As the cold-air mass flows over the ice edge over the relatively warm open ocean, intense turbulent heat and surface fluxes promote cloud formation. These clouds undergo a distinctive evolution from high-coverage stratiform decks to broken cumuliform cloud fields. These post-transition clouds typically have a much lower shortwave cooling effect due to their lower cloud fractions. Therefore, factors which may change the timing of the transition can change the role these clouds play in the Arctic energy budget. In particular, the presence of ice or frozen precipitation is thought to be key to the cloud evolution. However, the conditions influencing ice formation in these events are uncertain. Here, we have developed a method to observe the evolution of the cloud phase over time in these outbreaks and considered the role of air mass history on the cloud evolution.

After leaving the ice edge, MCAO clouds exhibit a rapid decline in the liquid phase, with a corresponding increase in mixed-phase clouds and some amount of glaciation into ice-only clouds (Fig. 1). In contrast, the liquid phase is persistently dominant in non-MCAO clouds, with particularly few ice-only clouds. The shift towards a more glaciated state in MCAO clouds is in agreement with previous in situ and measurement campaign observations (Abel et al., 2017; Lloyd et al., 2018; Mages et al., 2023), with higher amounts of ice found in the post-transition cumuliform clouds than in the original stratiform decks.

Mixed-phase clouds predominantly exist at low temperatures initially (around $-20\,°C$), gradually shifting to form at higher temperatures of around $-13\,°C$ (Fig. 2). In contrast, mixed-phase clouds form at higher temperatures in non-MCAOs very close to the ice edge. There is a seasonal dependence to the formation of ice in MCAOs and non-MCAOs (Figs. 5 and 6), with wintertime non-MCAO clouds only forming mixed phase at low temperatures initially and JJA MCAOs forming ice at $-13\,°C$ at the ice edge. These dif-

ferences in evolution appear to be related to air mass history; air masses which form MCAOs typically spend longer times over ice- and snow-covered surfaces, which usually are poor sources of INPs (Figs. 8 and 9). Therefore, the time taken to form mixed-phase clouds at higher temperatures appears to be associated with the transport of local, marine biological INPs to the cloud layer. In contrast, non-MCAO events typically spend less time over snow and ice and therefore may carry more INPs. Although the CAMS AOD data somewhat corroborate the results, with MCAO air parcels typically being cleaner, the difficulties in representing biological sources and INPs in models limit the utility of the reanalysis data. Despite several measurement campaigns, there is still considerable uncertainty about aerosol sources and sinks in the Arctic (Schmale et al., 2021). The results presented here highlight the need for more accurate measurements of the sources of biological INPs in the region, particularly close to the ice edge, and the mechanisms of transport to the cloud layer. Further knowledge of aerosol transportation pathways around the Arctic is also required, especially for understanding the seasonal differences in aerosol sources.

Further into the MCAO development, there is some evidence of mixed-phase clouds occurring with cloud top temperatures above $-10\,°C$ (Fig. 2). Although evidence of secondary ice production has previously been observed in MCAO clouds, particularly in regions of strong updrafts or high supercooled fraction (Abel et al., 2017; Mages et al., 2023), it is difficult to determine decisively with satellite data if the mechanism is ubiquitous. Karalis et al. (2022) showed that secondary ice formation was important for the development and break-up of MCAO clouds, particularly mechanisms such as drop-shattering and ice–ice collisional break-up. However, parameterizations of these mechanisms are highly uncertain and not widely implemented in climate models. Further laboratory and in situ studies are required to understand these mechanisms, which can improve the representation in the models and in turn help to understand whether or not secondary ice production contributes to the higher-temperature mixed-phase clouds observed in MCAOs.

This study provides evidence consistent with previous modelling work showing that MCAO cloud development is sensitive to INP concentration (Vergara-Temprado et al., 2018). Future changes in Arctic INP concentrations are expected to change the radiative properties of the clouds. Increasing temperatures mean that the Arctic is increasingly snow- and ice-free, therefore potentially making more INP sources more available for greater parts of the year (Ardyna et al., 2014). These increases in INPs may further increase the proportion of mixed-phase clouds in MCAOs, or help ice form earlier into the outbreak, and cause these clouds to break up more rapidly (Tornow et al., 2021). During polar day, both of these changes would decrease the cooling effects of the clouds, leading to a positive feedback. However, poor parameterizations of INPs in climate models, along with dif-

ficulties of modelling mixed-phase cloud properties and the dynamics of a complicated system like a MCAO, mean that understanding the impact of changes in aerosol concentrations is challenging. To accurately estimate the climate impact of this effect on a large scale, it is necessary to conduct detailed measurements of both aerosols and mixed-phase clouds across the Arctic.

References

Abel, S. J., Boutle, I. A., Waite, K., Fox, S., Brown, P. R. A., Cotton, R., Lloyd, G., Choularton, T. W., and Bower, K. N.: The Role of Precipitation in Controlling the Transition from Stratocumulus to Cumulus Clouds in a Northern Hemisphere Cold-Air Outbreak, J. Atmos. Sci., 74, 2293–2314, https://doi.org/10.1175/JAS-D-16-0362.1, 2017.

Aemisegger, F. and Papritz, L.: A Climatology of Strong Large-Scale Ocean Evaporation Events. Part I: Identification, Global Distribution, and Associated Climate Conditions, J. Climate, 31, 7287–7312, https://doi.org/10.1175/JCLI-D-17-0591.1, 2018.

Ardyna, M., Babin, M., Gosselin, M., Devred, E., Rainville, L., and Tremblay, J.-É.: Recent Arctic Ocean sea ice loss triggers novel fall phytoplankton blooms, Geophys. Res. Lett., 41, 6207–6212, https://doi.org/10.1002/2014GL061047, 2014.

Bigg, E. K.: Ice forming nuclei in the high Arctic, Tellus B, 48, 223–233, https://doi.org/10.3402/tellusb.v48i2.15888, 1996.

Bigg, E. K. and Leck, C.: Cloud-active particles over the central Arctic Ocean, J. Geophys. Res.-Atmos., 106, 32155–32166, https://doi.org/10.1029/1999JD901152, 2001.

Bodas-Salcedo, A., Williams, K., Ringer, M., Beau, I., Cole, J., Dufresne, J.-L., Koshiro, T., Stevens, B., Wang, Z., and Yokohata, T.: Origins of the solar radiation biases over the Southern Ocean in CFMIP2 models, J. Climate, 27, 41–56, https://doi.org/10.1175/JCLI-D-13-00169.1, 2014.

Bodas-Salcedo, A., Andrews, T., Karmalkar, A. V., and Ringer, M. A.: Cloud liquid water path and radiative feedbacks over the Southern Ocean, Geophys. Res. Lett., 43, 10938–10946, https://doi.org/10.1002/2016GL070770, 2016.

Brümmer, B.: Roll and Cell Convection in Wintertime Arctic Cold-Air Outbreaks, J. Atmos. Sci., 56, 2613–2636, https://doi.org/10.1175/1520-0469(1999)056<2613:RACCIW>2.0.CO;2, 1999.

Carlsen, T. and David, R. O.: Spaceborne Evidence That Ice-Nucleating Particles Influence High-Latitude Cloud Phase, Geophys. Res. Lett., 49, e2022GL098041, https://doi.org/10.1029/2022GL098041, 2022.

Cavalieri, D. J., Parkinson, C. L., Gloersen, P., and Zwally, H. J.: Sea Ice Concentrations from Nimbus-7 SMMR and DMSP SSM/I-SSMIS Passive Microwave Data, Version 1, Boulder, Colorado USA, NASA National Snow and Ice Data Center Distributed Active Archive Center [data set], https://doi.org/10.5067/8GQ8LZQVL0VL, 1996.

Ceccaldi, M., Delanoü, J., Hogan, R. J., Pounder, N. L., Protat, A., and Pelon, J.: From CloudSat-CALIPSO to EarthCare: Evolution of the DARDAR cloud classification and its comparison to airborne radar-lidar observations, J. Geophys. Res.-Atmos., 118, 7962–7981, https://doi.org/10.1002/jgrd.50579, 2013.

Cesana, G., Kay, J. E., Chepfer, H., English, J. M., and de Boer, G.: Ubiquitous low-level liquid-containing Arctic clouds: New observations and climate model constraints from CALIPSO-GOCCP, Geophys. Res. Lett., 39, L20804, https://doi.org/10.1029/2012GL053385, 2012.

Cesana, G. V., Khadir, T., Chepfer, H., and Chiriaco, M.: Southern Ocean Solar Reflection Biases in CMIP6 Models Linked to Cloud Phase and Vertical Structure Representations, Geophys. Res. Lett., 49, e2022GL099777, https://doi.org/10.1029/2022GL099777, 2022.

Christensen, M. W., Chen, Y.-C., and Stephens, G. L.: Aerosol indirect effect dictated by liquid clouds, J. Geophys. Res.-Atmos., 121, 14636–14650, https://doi.org/10.1002/2016JD025245, 2016.

Creamean, J. M., Cross, J. N., Pickart, R., McRaven, L., Lin, P., Pacini, A., Hanlon, R., Schmale, D. G., Ceniceros, J., Aydell, T., Colombi, N., Bolger, E., and DeMott, P. J.: Ice Nucleating Particles Carried From Below a Phytoplankton Bloom to the Arctic Atmosphere, Geophys. Res. Lett., 46, 8572–8581, https://doi.org/10.1029/2019GL083039, 2019.

Creamean, J. M., Barry, K., Hill, T. C. J., Hume, C., DeMott, P. J., Shupe, M. D., Dahlke, S., Willmes, S., Schmale, J., Beck, I., Hoppe, C. J. M., Fong, A., Chamberlain, E., Bowman, J., Scharien, R., and Persson, O.: Annual cycle observations of aerosols capable of ice formation in central Arctic clouds, Nat. Commun., 13, 3537, https://doi.org/10.1038/s41467-022-31182-x, 2022.

D'Alessandro, J. J., McFarquhar, G. M., Wu, W., Stith, J. L., Jensen, J. B., and Rauber, R. M.: Characterizing the Occurrence and Spatial Heterogeneity of Liquid, Ice, and Mixed Phase Low-Level Clouds Over the Southern Ocean Using in Situ Observations Acquired During SOCRATES, J. Geophys. Res.-Atmos., 126, e2020JD034482, https://doi.org/10.1029/2020JD034482, 2021.

Danker, J., Sourdeval, O., McCoy, I. L., Wood, R., and Possner, A.: Exploring relations between cloud morphology, cloud phase, and cloud radiative properties in Southern Ocean's stratocumulus clouds, Atmos. Chem. Phys., 22, 10247–10265, https://doi.org/10.5194/acp-22-10247-2022, 2022.

de Boer, G., Morrison, H., Shupe, M. D., and Hildner, R.: Evidence of liquid dependent ice nucleation in high-latitude stratiform clouds from surface remote sensors, Geophys. Res. Lett., 38, L01803, https://doi.org/10.1029/2010GL046016, 2011.

Delanoë, J. and Hogan, R. J.: Combined CloudSat-CALIPSO-MODIS retrievals of the properties of ice clouds, J. Geophys. Res.-Atmos., 115, D00H29, https://doi.org/10.1029/2009JD012346, 2010.

DiGirolamo, N., Parkinson, C. L., Cavalieri, D. J., Gloersen, P., and Zwally, H. J.: Sea Ice Concentrations from Nimbus-7 SMMR and DMSP SSM/I-SSMIS Passive Microwave Data, Version 2, NSIDC [data set], https://doi.org/10.5067/MPYG15WAA4WX, 2022.

Field, P. R., Cotton, R. J., McBeath, K., Lock, A. P., Webster, S., and Allan, R. P.: Improving a convection-permitting model simulation of a cold air outbreak, Q. J. Roy. Meteor. Soc., 140, 124–138, https://doi.org/10.1002/qj.2116, 2014.

Field, P. R., Brožková, R., Chen, M., Dudhia, J., Lac, C., Hara, T., Honnert, R., Olson, J., Siebesma, P., de Roode, S., Tomassini, L., Hill, A., and McTaggart-Cowan, R.: Exploring the convective grey zone with regional simulations of a cold air outbreak, Q. J. Roy. Meteor. Soc., 143, 2537–2555, https://doi.org/10.1002/qj.3105, 2017.

Fletcher, J., Mason, S., and Jakob, C.: The Climatology, Meteorology, and Boundary Layer Structure of Marine Cold Air Outbreaks in Both Hemispheres, J. Climate, 29, 1999–2014, https://doi.org/10.1175/JCLI-D-15-0268.1, 2016a.

Fletcher, J. K., Mason, S., and Jakob, C.: A Climatology of Clouds in Marine Cold Air Outbreaks in Both Hemispheres, J. Climate, 29, 6677–6692, https://doi.org/10.1175/JCLI-D-15-0783.1, 2016b.

Geerts, B., Pokharel, B., and Kristovich, D. A. R.: Blowing Snow as a Natural Glaciogenic Cloud Seeding Mechanism, Mon. Weather Rev., 143, 5017–5033, https://doi.org/10.1175/MWR-D-15-0241.1, 2015.

Geerts, B., Giangrande, S. E., McFarquhar, G. M., Xue, L., Abel, S. J., Comstock, J. M., Crewell, S., DeMott, P. J., Ebell, K., Field, P., Hill, T. C. J., Hunzinger, A., Jensen, M. P., Johnson, K. L., Juliano, T. W., Kollias, P., Kosovic, B., Lackner, C., Luke, E., Lüpkes, C., Matthews, A. A., Neggers, R., Ovchinnikov, M., Powers, H., Shupe, M. D., Spengler, T., Swanson, B. E., Tjernström, M., Theisen, A. K., Wales, N. A., Wang, Y., Wendisch, M., and Wu, P.: The COMBLE campaign: a study of marine boundary-layer clouds in Arctic cold-air outbreaks, B. Am. Meteorol. Soc., 103, E1371–E1389, https://doi.org/10.1175/BAMS-D-21-0044.1, 2022.

Grosvenor, D. P. and Wood, R.: The effect of solar zenith angle on MODIS cloud optical and microphysical retrievals within marine liquid water clouds, Atmos. Chem. Phys., 14, 7291–7321, https://doi.org/10.5194/acp-14-7291-2014, 2014.

Hallett, J. and Mossop, S.: Production of secondary ice particles during the riming process, Nature, 249, 26–28, https://doi.org/10.1038/249026a0, 1974.

Hartmann, J., Kottmeier, C., and Raasch, S.: Roll Vortices and Boundary-Layer Development during a Cold Air Outbreak, Bound.-Lay. Meteorol., 84, 45–65, https://doi.org/10.1023/A:1000392931768, 1997.

Hartmann, M., Adachi, K., Eppers, O., Haas, C., Herber, A., Holzinger, R., Hünerbein, A., Jäkel, E., Jentzsch, C., van Pinxteren, M., Wex, H., Willmes, S., and Stratmann, F.: Wintertime Airborne Measurements of Ice Nucleating Particles in the High Arctic: A Hint to a Marine, Biogenic Source for Ice Nucleating Particles, Geophys. Res. Lett., 47, e2020GL087770, https://doi.org/10.1029/2020GL087770, 2020.

Hartmann, M., Gong, X., Kecorius, S., van Pinxteren, M., Vogl, T., Welti, A., Wex, H., Zeppenfeld, S., Herrmann, H., Wiedensohler, A., and Stratmann, F.: Terrestrial or marine – indications towards the origin of ice-nucleating particles during melt season in the European Arctic up to 83.7° N, Atmos. Chem. Phys., 21, 11613–11636, https://doi.org/10.5194/acp-21-11613-2021, 2021.

Hersbach, H., Bell, B., Berrisford, P., Hirahara, S., Horányi, A., Muñoz-Sabater, J., Nicolas, J., Peubey, C., Radu, R., Schepers, D., Simmons, A., Soci, C., Abdalla, S., Abellan, X., Balsamo, G., Bechtold, P., Biavati, G., Bidlot, J., Bonavita, M., De Chiara, G., Dahlgren, P., Dee, D., Diamantakis, M., Dragani, R., Flemming, J., Forbes, R., Fuentes, M., Geer, A., Haimberger, L., Healy, S., Hogan, R. J., Hólm, E., Janisková, M., Keeley, S., Laloyaux, P., Lopez, P., Lupu, C., Radnoti, G., de Rosnay, P., Rozum, I., Vamborg, F., Villaume, S., and Thépaut, J.-N.: The ERA5 global reanalysis, Q. J. Roy. Meteor. Soc., 146, 1999–2049, https://doi.org/10.1002/qj.3803, 2020 (data available at: https://cds.climate.copernicus.eu/cdsapp#!/dataset/reanalysis-era5-complete, last access: February 2024).

Heymsfield, A. J. and Mossop, S. C.: Temperature dependence of secondary ice crystal production during soft hail growth by riming, Q. J. Roy. Meteor. Soc., 110, 765–770, https://doi.org/10.1002/qj.49711046512, 1984.

Horner, G. and Gryspeerdt, E.: The evolution of deep convective systems and their associated cirrus outflows, Atmos. Chem. Phys., 23, 14239–14253, https://doi.org/10.5194/acp-23-14239-2023, 2023.

Inness, A., Ades, M., Agustí-Panareda, A., Barré, J., Benedictow, A., Blechschmidt, A.-M., Dominguez, J. J., Engelen, R., Eskes, H., Flemming, J., Huijnen, V., Jones, L., Kipling, Z., Massart, S., Parrington, M., Peuch, V.-H., Razinger, M., Remy, S., Schulz, M., and Suttie, M.: The CAMS reanalysis of atmospheric composition, Atmos. Chem. Phys., 19, 3515–3556, https://doi.org/10.5194/acp-19-3515-2019, 2019 (data available at: https://ads.atmosphere.copernicus.eu/cdsapp#!/dataset/cams-global-reanalysis-eac4, last access: November 2023).

Inoue, J., Tobo, Y., Taketani, F., and Sato, K.: Oceanic Supply of Ice-Nucleating Particles and Its Effect on Ice Cloud Formation: A Case Study in the Arctic Ocean During a Cold-Air Outbreak in Early Winter, Geophys. Res. Lett., 48, e2021GL094646, https://doi.org/10.1029/2021GL094646, 2021.

IPCC: Climate Change: The Physical Science Basis. Contribution of Working Group I to the Sixth Assessment Report of the Intergovernmen- tal Panel on Climate Change, edited by: Masson-Delmotte, V., Zhai, P., Pirani, A., Connors, S. L., Péan, C., Berger, S., Caud, N., Chen, Y., Goldfarb, L., Gomis, M. I., Huang, M., Leitzell, K., Lonnoy, E., Matthews, J. B. R., Maycock, T. K., Waterfield, T., Yelekçi, O., Yu, R., and Zhou, B., Cambridge University Press, Cambridge, United Kingdom and New York, NY, US, 2215–2256, https://doi.org/10.1017/9781009157896.022, 2021.

Irish, V. E., Elizondo, P., Chen, J., Chou, C., Charette, J., Lizotte, M., Ladino, L. A., Wilson, T. W., Gosselin, M., Murray, B. J., Polishchuk, E., Abbatt, J. P. D., Miller, L. A., and Bertram, A. K.: Ice-nucleating particles in Canadian Arctic sea-surface microlayer and bulk seawater, Atmos. Chem. Phys., 17, 10583–10595, https://doi.org/10.5194/acp-17-10583-2017, 2017.

Irish, V. E., Hanna, S. J., Willis, M. D., China, S., Thomas, J. L., Wentzell, J. J. B., Cirisan, A., Si, M., Leaitch, W. R., Murphy, J. G., Abbatt, J. P. D., Laskin, A., Girard, E., and Bertram, A. K.: Ice nucleating particles in the marine boundary layer in the Canadian Arctic during summer 2014, Atmos. Chem. Phys., 19, 1027–1039, https://doi.org/10.5194/acp-19-1027-2019, 2019.

Karalis, M., Sotiropoulou, G., Abel, S. J., Bossioli, E., Georgakaki, P., Methymaki, G., Nenes, A., and Tombrou, M.: Effects of secondary ice processes on a stratocumulus to cumulus transition during a cold-air outbreak, Atmos. Res., 277, 106302, https://doi.org/10.1016/j.atmosres.2022.106302, 2022.

Kay, J. E. and Gettelman, A.: Cloud influence on and response to seasonal Arctic sea ice loss, J. Geophys. Res.-Atmos., 114, D18204, https://doi.org/10.1029/2009JD011773, 2009.

Khanal, S. and Wang, Z.: Uncertainties in MODIS-Based Cloud Liquid Water Path Retrievals at High Latitudes Due to Mixed-Phase Clouds and Cloud Top Height Inhomogeneity, J. Geophys. Res.-Atmos., 123, 11154–11172, https://doi.org/10.1029/2018JD028558, 2018.

Kolstad, E. W.: Higher ocean wind speeds during marine cold air outbreaks, Q. J. Roy. Meteor. Soc., 143, 2084–2092, https://doi.org/10.1002/qj.3068, 2017.

Kolstad, E. W. and Bracegirdle, T. J.: Marine cold-air outbreaks in the future: an assessment of IPCC AR4 model results for the Northern Hemisphere, Clim. Dynam., 30, 871–885, https://doi.org/10.1007/s00382-007-0331-0, 2008.

Kolstad, E. W., Bracegirdle, T. J., and Seierstad, I. A.: Marine cold-air outbreaks in the North Atlantic: temporal distribution and associations with large-scale atmospheric circulation, Clim. Dynam., 33, 187–197, https://doi.org/10.1007/s00382-008-0431-5, 2009.

Korolev, A., Heckman, I., Wolde, M., Ackerman, A. S., Fridlind, A. M., Ladino, L. A., Lawson, R. P., Milbrandt, J., and Williams, E.: A new look at the environmental conditions favorable to secondary ice production, Atmos. Chem. Phys., 20, 1391–1429, https://doi.org/10.5194/acp-20-1391-2020, 2020.

Korolev, A. V., Isaac, G. A., Cober, S. G., Strapp, J. W., and Hallett, J.: Microphysical characterization of mixed-phase clouds, Q. J. Roy. Meteor. Soc., 129, 39–65, https://doi.org/10.1256/qj.01.204, 2003.

Lackner, C. P., Geerts, B., Wang, Y., Juliano, T. W., Xue, L., Kosović, B., and Turner, D. D.: Insights into the relation between vertical cloud structure and dynamics of three polar lows: Observations from COMBLE, Q. J. Roy. Meteor. Soc., 149, 2992–3013, https://doi.org/10.1002/qj.4543, 2023.

Lensky, I. M. and Rosenfeld, D.: The time-space exchangeability of satellite retrieved relations between cloud top temperature and particle effective radius, Atmos. Chem. Phys., 6, 2887–2894, https://doi.org/10.5194/acp-6-2887-2006, 2006.

Li, G., Wilbourn, E. K., Cheng, Z., Wieder, J., Fagerson, A., Henneberger, J., Motos, G., Traversi, R., Brooks, S. D., Mazzola, M., China, S., Nenes, A., Lohmann, U., Hiranuma, N., and Kanji, Z. A.: Physicochemical characterization and source apportionment of Arctic ice-nucleating particles observed in Ny-Ålesund in autumn 2019, Atmos. Chem. Phys., 23, 10489–10516, https://doi.org/10.5194/acp-23-10489-2023, 2023.

Li, X., Krueger, S., Strong, C., Mace, G., and Benson, S.: Midwinter Arctic leads form and dissipate low clouds, Nat. Commun., 11, 206, https://doi.org/10.1038/s41467-019-14074-5, 2020.

Lindsay, R. W. and Rothrock, D. A.: Arctic sea ice leads from advanced very high resolution radiometer images, J. Geophys. Res.-Oceans, 100, 4533–4544, https://doi.org/10.1029/94JC02393, 1995.

Lloyd, G., Choularton, T. W., Bower, K. N., Gallagher, M. W., Crosier, J., O'Shea, S., Abel, S. J., Fox, S., Cotton, R., and Boutle, I. A.: In situ measurements of cloud microphysical and aerosol properties during the break-up of stratocumulus cloud layers in cold air outbreaks over the North Atlantic, Atmos. Chem. Phys., 18, 17191–17206, https://doi.org/10.5194/acp-18-17191-2018, 2018.

Luke, E., Yang, F., Kollias, P., Vogelmann, A., and Maahn, M.: New insights into ice multiplication using remote-sensing observations of slightly supercooled mixed-phase clouds in the Arctic, P. Natl. Acad. Sci. USA, 118, e2021387118, https://doi.org/10.1073/pnas.2021387118, 2021.

Mages, Z., Kollias, P., Zhu, Z., and Luke, E. P.: Surface-based observations of cold-air outbreak clouds during the COMBLE field campaign, Atmos. Chem. Phys., 23, 3561–3574, https://doi.org/10.5194/acp-23-3561-2023, 2023.

Mann, H. B. and Whitney, D. R.: On a Test of Whether one of Two Random Variables is Stochastically Larger than the Other, Ann. Math. Stat., 18, 50–60, https://doi.org/10.1214/aoms/1177730491, 1947.

Marchand, R., Mace, G. G., Ackerman, T., and Stephens, G.: Hydrometeor Detection Using *Cloudsat* – An Earth-Orbiting 94-GHz Cloud Radar, J. Atmos. Ocean. Tech., 25, 519–533, https://doi.org/10.1175/2007JTECHA1006.1, 2008.

Marchant, B., Platnick, S., Meyer, K., Arnold, G. T., and Riedi, J.: MODIS Collection 6 shortwave-derived cloud phase classification algorithm and comparisons with CALIOP, Atmos. Meas. Tech., 9, 1587–1599, https://doi.org/10.5194/amt-9-1587-2016, 2016.

Mateling, M. E., Pettersen, C., Kulie, M. S., and L'Ecuyer, T. S.: Marine Cold-Air Outbreak Snowfall in the North Atlantic: A CloudSat Perspective, J. Geophys. Res.-Atmos., 128, e2022JD038053, https://doi.org/10.1029/2022JD038053, 2023.

Mauritsen, T., Sedlar, J., Tjernström, M., Leck, C., Martin, M., Shupe, M., Sjogren, S., Sierau, B., Persson, P. O. G., Brooks, I. M., and Swietlicki, E.: An Arctic CCN-limited cloud-aerosol regime, Atmos. Chem. Phys., 11, 165–173, https://doi.org/10.5194/acp-11-165-2011, 2011.

McCluskey, C. S., Hill, T. C. J., Sultana, C. M., Laskina, O., Trueblood, J., Santander, M. V., Beall, C. M., Michaud, J. M., Kreidenweis, S. M., Prather, K. A., Grassian, V., and DeMott, P. J.: A Mesocosm Double Feature: Insights into the Chemical Makeup of Marine Ice Nucleating Particles, J. Atmos. Sci., 75, 2405–2423, https://doi.org/10.1175/JAS-D-17-0155.1, 2018.

McCoy, I. L., Wood, R., and Fletcher, J. K.: Identifying Meteorological Controls on Open and Closed Mesoscale Cellular Convection Associated with Marine Cold Air Outbreaks, J. Geophys. Res.-Atmos., 122, 11678–11702, https://doi.org/10.1002/2017JD027031, 2017.

McErlich, C., McDonald, A., Schuddeboom, A., and Silber, I.: Comparing Satellite- and Ground-Based Observations of Cloud Occurrence Over High Southern Latitudes, J. Geophys. Res.-Atmos., 126, e2020JD033607, https://doi.org/10.1029/2020JD033607, 2021.

Morrison, H., de Boer, G., Feingold, G., Harrington, J., Shupe, M. D., and Sulia, K.: Resilience of persistent Arctic mixed-phase clouds, Nat. Geosci., 5, 11–17, https://doi.org/10.1038/ngeo1332, 2012.

Mossop, S. C.: The influence of drop size distribution on the production of secondary ice particles during graupel growth, Q. J. Roy. Meteor. Soc., 104, 323–330, https://doi.org/10.1002/qj.49710444007, 1978.

Mossop, S. C.: Secondary ice particle production during rime growth: The effect of drop size distribution and rimer velocity, Q. J. Roy. Meteor. Soc., 111, 1113–1124, https://doi.org/10.1002/qj.49711147012, 1985.

Murray, B. J., O'Sullivan, D., Atkinson, J. D., and Webb, M. E.: Ice nucleation by particles immersed in supercooled cloud droplets, Chem. Soc. Rev., 41, 6519–6554, https://doi.org/10.1039/C2CS35200A, 2012.

Murray, B. J., Carslaw, K. S., and Field, P. R.: Opinion: Cloud-phase climate feedback and the importance of ice-nucleating particles, Atmos. Chem. Phys., 21, 665–679, https://doi.org/10.5194/acp-21-665-2021, 2021.

Murray-Watson, R. J., Gryspeerdt, E., and Goren, T.: Investigating the development of clouds within marine cold-air outbreaks, Atmos. Chem. Phys., 23, 9365–9383, https://doi.org/10.5194/acp-23-9365-2023, 2023.

Papritz, L. and Spengler, T.: A Lagrangian Climatology of Wintertime Cold Air Outbreaks in the Irminger and Nordic Seas and

Their Role in Shaping Air-Sea Heat Fluxes, J. Climate, 30, 2717–2737, https://doi.org/10.1175/JCLI-D-16-0605.1, 2017.

Partain, P.: Cloudsat ECMWF-AUX auxiliary data process description and interface control document, https://www.cloudsat.cira.colostate.edu/cloudsat-static/info/dl/ecmwf-aux/ECMWF-AUX.PDICD.P1_R05.rev0.pdf (last access: 1 November 2023), 2022.

Pereira Freitas, G., Adachi, K., Conen, F., Heslin-Rees, D., Krejci, R., Tobo, Y., Espen Yttri, K., and Zieger, P.: Regionally sourced bioaerosols drive high-temperature ice nucleating particles in the Arctic, Nat. Commun., 14, 5997, https://doi.org/10.1038/s41467-023-41696-7, 2023.

Pithan, F., Svensson, G., Caballero, R., Chechin, D., Cronin, T. W., Ekman, A. M. L., Neggers, R., Shupe, M. D., Solomon, A., Tjernström, M., and Wendisch, M.: Role of air-mass transformations in exchange between the Arctic and mid-latitudes, Nat. Geosci., 11, 805–812, https://doi.org/10.1038/s41561-018-0234-1, 2018.

Platnick, S., Meyer, K. G., King, M. D., Wind, G., Amarasinghe, N., Marchant, B., Arnold, G. T., Zhang, Z., Hubanks, P. A., Holz, R. E., Yang, P., Ridgway, W. L., and Riedi, J.: The MODIS Cloud Optical and Microphysical Products: Collection 6 Updates and Examples From Terra and Aqua, IEEE T. Geosci. Remote, 55, 502–525, https://doi.org/10.1109/TGRS.2016.2610522, 2017 (data available at: https://modis.gsfc.nasa.gov/data/dataprod/mod06.php, last access: June 2022).

Porter, G. C. E., Adams, M. P., Brooks, I. M., Ickes, L., Karlsson, L., Leck, C., Salter, M. E., Schmale, J., Siegel, K., Sikora, S. N. F., Tarn, M. D., Vüllers, J., Wernli, H., Zieger, P., Zinke, J., and Murray, B. J.: Highly Active Ice-Nucleating Particles at the Summer North Pole, J. Geophys. Res.-Atmos., 127, e2021JD036059, https://doi.org/10.1029/2021JD036059, 2022.

Rangno, A. L. and Hobbs, P. V.: Ice particles in stratiform clouds in the Arctic and possible mechanisms for the production of high ice concentrations, J. Geophys. Res.-Atmos., 106, 15065–15075, https://doi.org/10.1029/2000JD900286, 2001.

Renfrew, I. A. and Moore, G. W. K.: An Extreme Cold-Air Outbreak over the Labrador Sea: Roll Vortices and Air-Sea Interaction, Mon. Weather Rev., 127, 2379–2394, https://doi.org/10.1175/1520-0493(1999)127<2379:AECAOO>2.0.CO;2, 1999.

Rosenfeld, D. and Gutman, G.: Retrieving microphysical properties near the tops of potential rain clouds by multispectral analysis of AVHRR data, Atmos. Res., 34, 259–283, https://doi.org/10.1016/0169-8095(94)90096-5, 1994.

Rosenfeld, D., Yu, X., Liu, G., Xu, X., Zhu, Y., Yue, Z., Dai, J., Dong, Z., Dong, Y., and Peng, Y.: Glaciation temperatures of convective clouds ingesting desert dust, air pollution and smoke from forest fires, Geophys. Res. Lett., 38, L21804, https://doi.org/10.1029/2011GL049423, 2011.

Schirmacher, I., Kollias, P., Lamer, K., Mech, M., Pfitzenmaier, L., Wendisch, M., and Crewell, S.: Assessing Arctic low-level clouds and precipitation from above – a radar perspective, Atmos. Meas. Tech., 16, 4081–4100, https://doi.org/10.5194/amt-16-4081-2023, 2023.

Schmale, J., Zieger, P., and Ekman, A.: Aerosols in current and future Arctic climate, Nat. Clim. Change, 11, 95–105, https://doi.org/10.1038/s41558-020-00969-5, 2021.

Seethala, C. and Horváth, Á.: Global assessment of AMSR-E and MODIS cloud liquid water path retrievals in warm oceanic clouds, J. Geophys. Res.-Atmos., 115, D13202, https://doi.org/10.1029/2009JD012662, 2010.

Shapiro, M. A., Fedor, L. S., and Hampel, T.: Research aircraft measurements of a polar low over the Norwegian Sea, Tellus A, 39, 272–306, https://doi.org/10.3402/tellusa.v39i4.11761, 1987.

Shupe, M. D.: Clouds at Arctic Atmospheric Observatories. Part II: Thermodynamic Phase Characteristics, J. Appl. Meteorol. Clim., 50, 645–661, https://doi.org/10.1175/2010JAMC2468.1, 2011.

Shupe, M. D. and Intrieri, J. M.: Cloud Radiative Forcing of the Arctic Surface: The Influence of Cloud Properties, Surface Albedo, and Solar Zenith Angle, J. Climate, 17, 616–628, https://doi.org/10.1175/1520-0442(2004)017<0616:CRFOTA>2.0.CO;2, 2004.

Shupe, M. D., Matrosov, S. Y., and Uttal, T.: Arctic Mixed-Phase Cloud Properties Derived from Surface-Based Sensors at SHEBA, J. Atmos. Sci., 63, 697–711, https://doi.org/10.1175/JAS3659.1, 2006.

Silber, I. and Shupe, M. D.: Insights on sources and formation mechanisms of liquid-bearing clouds over MOSAiC examined from a Lagrangian framework, Elementa: Science of the Anthropocene, 10, 000071, https://doi.org/10.1525/elementa.2021.000071, 2022.

Silber, I., Fridlind, A. M., Verlinde, J., Ackerman, A. S., Chen, Y.-S., Bromwich, D. H., Wang, S.-H., Cadeddu, M., and Eloranta, E. W.: Persistent Supercooled Drizzle at Temperatures Below $-25\,°C$ Observed at McMurdo Station, Antarctica, J. Geophys. Res.-Atmos., 124, 10878–10895, https://doi.org/10.1029/2019JD030882, 2019.

Stephens, G. L., Vane, D. G., Tanelli, S., Im, E., Durden, S., Rokey, M., Reinke, D., Partain, P., Mace, G. G., Austin, R., L'Ecuyer, T., Haynes, J., Lebsock, M., Suzuki, K., Waliser, D., Wu, D., Kay, J., Gettelman, A., Wang, Z., and Marchand, R.: CloudSat mission: Performance and early science after the first year of operation, J. Geophys. Res.-Atmos., 113, D00A18, https://doi.org/10.1029/2008JD009982, 2008.

Sullivan, S. C., Hoose, C., Kiselev, A., Leisner, T., and Nenes, A.: Initiation of secondary ice production in clouds, Atmos. Chem. Phys., 18, 1593–1610, https://doi.org/10.5194/acp-18-1593-2018, 2018.

Tan, I. and Storelvmo, T.: Evidence of Strong Contributions From Mixed-Phase Clouds to Arctic Climate Change, Geophys. Res. Lett., 46, 2894–2902, https://doi.org/10.1029/2018GL081871, 2019.

Tornow, F., Ackerman, A. S., and Fridlind, A. M.: Preconditioning of overcast-to-broken cloud transitions by riming in marine cold air outbreaks, Atmos. Chem. Phys., 21, 12049–12067, https://doi.org/10.5194/acp-21-12049-2021, 2021.

U.S. National Ice Center: IMS Daily Northern Hemisphere Snow and Ice Analysis at 1 km, 4 km, and 24 km Resolutions, Version 1, National Snow and Ice Data Center [data set], https://doi.org/10.7265/N52R3PMC, 2008.

Van Weverberg, K., Giangrande, S., Zhang, D., Morcrette, C. J., and Field, P. R.: On the Role of Macrophysics and Microphysics in Km-Scale Simulations of Mixed-Phase Clouds During Cold Air Outbreaks, J. Geophys. Res.-Atmos., 128, e2022JD037854, https://doi.org/10.1029/2022JD037854, 2023.

Vergara-Temprado, J., Miltenberger, A. K., Furtado, K., Grosvenor, D. P., Shipway, B. J., Hill, A. A., Wilkinson, J. M., Field, P. R., Murray, B. J., and Carslaw, K. S.: Strong control of Southern Ocean Cloud reflectivity by ice-nucleating particles, P. Natl. Acad. Sci. USA, 115, 2687–2692, 2018.

Wadhams, P., McLaren, A. S., and Weintraub, R.: Ice thickness distribution in Davis Strait in February from submarine sonar profiles, J. Geophys. Res.-Oceans, 90, 1069–1077, https://doi.org/10.1029/JC090iC01p01069, 1985.

Wang, Q., Danilov, S., Jung, T., Kaleschke, L., and Wernecke, A.: Sea ice leads in the Arctic Ocean: Model assessment, interannual variability and trends, Geophys. Res. Lett., 43, 7019–7027, https://doi.org/10.1002/2016GL068696, 2016a.

Wang, T., Fetzer, E. J., Wong, S., Kahn, B. H., and Yue, Q.: Validation of MODIS cloud mask and multilayer flag using CloudSat-CALIPSO cloud profiles and a cross-reference of their cloud classifications, J. Geophys. Res.-Atmos., 121, 11620–11635, https://doi.org/10.1002/2016JD025239, 2016b.

Westbrook, C. D. and Illingworth, A. J.: Evidence that ice forms primarily in supercooled liquid clouds at temperatures $> -27\,°C$, Geophys. Res. Lett., 38, L14808, https://doi.org/10.1029/2011GL048021, 2011.

Wex, H., Huang, L., Zhang, W., Hung, H., Traversi, R., Becagli, S., Sheesley, R. J., Moffett, C. E., Barrett, T. E., Bossi, R., Skov, H., Hünerbein, A., Lubitz, J., Löffler, M., Linke, O., Hartmann, M., Herenz, P., and Stratmann, F.: Annual variability of ice-nucleating particle concentrations at different Arctic locations, Atmos. Chem. Phys., 19, 5293–5311, https://doi.org/10.5194/acp-19-5293-2019, 2019.

Wilson, T. W., Ladino, L. A., Alpert, P. A., Breckels, M. N., Brooks, I. M., Browse, J., Burrows, S. M., Carslaw, K. S., Huffman, J. A., Judd, C., Kilthau, W. P., Mason, R. H., McFiggans, G., Miller, L. A., Nájera, J. J., Polishchuk, E., Rae, S., Schiller, C. L., Si, M., Vergara Temprado, J., Whale, T. F., Wong, J. P. S., Wurl, O., Yakobi-Hancock, J. D., Abbatt, J. P. D., Aller, J. Y., Bertram, A. K., Knopf, D. A., and Murray, B. J.: A marine biogenic source of atmospheric ice-nucleating particles, Nature, 525, 234–238, https://doi.org/10.1038/nature14986, 2015.

Winker, D. M., Vaughan, M. A., Omar, A., Hu, Y., Powell, K. A., Liu, Z., Hunt, W. H., and Young, S. A.: Overview of the CALIPSO Mission and CALIOP Data Processing Algorithms, J. Atmos. Ocean. Tech., 26, 2310–2323, https://doi.org/10.1175/2009JTECHA1281.1, 2009.

Yamaguchi, T., Feingold, G., and Kazil, J.: Stratocumulus to Cumulus Transition by Drizzle, J. Adv. Model. Earth Sy., 9, 2333–2349, https://doi.org/10.1002/2017MS001104, 2017.

Yan, Y., Liu, X., Liu, Y., and Lu, J.: Comparison of mixed-phase clouds over the Arctic and the Tibetan Plateau: seasonality and vertical structure of cloud radiative effects, Clim. Dynam., 54, 4811–4822, https://doi.org/10.1007/s00382-020-05257-8, 2020.

Zhang, D., Wang, Z., Luo, T., Yin, Y., and Flynn, C.: The occurrence of ice production in slightly supercooled Arctic stratiform clouds as observed by ground-based remote sensors at the ARM NSA site, J. Geophys. Res.-Atmos., 122, 2867–2877, https://doi.org/10.1002/2016JD026226, 2017.

Zhang, D., Wang, Z., Kollias, P., Vogelmann, A. M., Yang, K., and Luo, T.: Ice particle production in mid-level stratiform mixed-phase clouds observed with collocated A-Train measurements, Atmos. Chem. Phys., 18, 4317–4327, https://doi.org/10.5194/acp-18-4317-2018, 2018.

Zhang, Z. and Platnick, S.: An assessment of differences between cloud effective particle radius retrievals for marine water clouds from three MODIS spectral bands, J. Geophys. Res.-Atmos., 116, D20215, https://doi.org/10.1029/2011JD016216, 2011.